2022 IEEE International Multi-Conference on Engineering, Computer and Information Sciences (SIBIRCON) | 978-1-6654-6480-2/22/$31.00 ©2022 IEEE | DOI: 10.1109/SIBIRCON56155.2022.10017008

# Synthesizing of Ultra-Wide Band Impulse by means of a Log-Periodic Dipole Antenna. Case Study for a Radar Stand Experiment

Konstantin Muzalevskiy
*Laboratory of Radiophysics of the Earth Remote Sensing*
*Kirensky Institute of Physics Federal Research Center KSC Siberian Branch Russian Academy of Science*
Krasnoyarsk, The Russian Federation
email: rsdkm@ksc.krasn.ru

Mikhail Mikhaylov
*Laboratory of Radiophysics of the Earth Remote Sensing*
*Kirensky Institute of Physics Federal Research Center KSC Siberian Branch Russian Academy of Science*
Krasnoyarsk, The Russian Federation
email: fractaloff@mail.ru

Zdenek Ruzicka
*Laboratory of Radiophysics of the Earth Remote Sensing*
*Kirensky Institute of Physics Federal Research Center KSC Siberian Branch Russian Academy of Science*
Krasnoyarsk, The Russian Federation
email: rsdzr@ksc.krasn.ru

***Abstract*—In this work, the approach of ultra-wide band pulses synthesizing is proposed using a broadband low-cost log-periodic dipole antenna and a vector network analyzer. Synthesis of UWB pulse (duration of 2.2ns) became possible due to minimization of antenna dispersion by compensation of amplitude and phase-frequency distortions introduced by the antenna into radiated and received pulse. The method had been developed for a down-looking antenna in a monostatic radar configuration. The antenna return loss was calculated using the model of two-port linear network with S-parameters. To calibrate the model, an original amplitude-phase method was proposed that requires measuring the antenna's return loss when the antenna is located only at several heights above the reflecting surface (metal sheet). In this case, the antenna return loss in an empty room does not need to be measured. The proposed method for synthesizing UWB pulses does not require changes in the design of the antenna and can be implemented as an additional software calibration of the antenna-feeder path. The proposed method of UWB pulses synthesizing can be implemented using miniature, low-cost vector network analyzers for environment remote sensing from unmanned aerial vehicle using the UWB impulses.**

***Keywords—Microwave remote sensing, log-periodic dipole antenna, calibration antenna, complex antenna transfer function, ultra-wide band impulse, radiation and receiving impulse***

## I. INTRODUCTION

With the development and use of ground penetration radar systems on lightweight unmanned aerial vehicle (UAV) platforms are concerned very recent promising advances regarding soil moisture mapping [1] and landmine detection [2]-[4]. Most often as miniaturized UAV radar systems uses the commercially available [5] or specially manufactured [2], portable stepped-frequency continuous-wave (SFCW) radars. These modern portable SFCW radars have compact size, high signal-to-noise ratio, the efficient use of power and sampling with a low-cost analog to digital converter (in comparison with pulsed radars) [6]. However, one of the significant disadvantages of SFCW is the low switching speed between frequencies (limited by the frequency synthesizers, which need a certain time to lock a frequency) [2]. The time measurement at one frequency (dwell time) of modern compact SFCW radars is in the range of ~ 100-200 μs [5], [6], and the total number of frequency samples depends on the width of radiation spectrum and the duration of sweep in the time domain. Due to the finite dwell time during scans of frequencies, significant changes in the reflective properties of the radar footprint area can occur as an UAV moves. As a result, the coherence conditions between transmitted (received) signals at different frequencies during scanning can be violated, which can increase the sidelobes level in a time-domain or almost destroy the signal. The limitation can be solved: i) in the hardware by adding parallel frequency synthesizers, ii) lowering the number of frequency steps, but this would increase the level of impulse sidelobes in time-base.

The unevenness of amplitude and phase-frequency characteristics of the radar's antennas are additional distortions in the spectrum of transmitted and received impulses introduce. Mainly, broadband log-periodic dipole (LPD) antennas, Vivaldi or Vivaldi-horn antennas are used as transmitting and receiving antennas on UAVs. LPD antennas have significant frequency dispersion of transfer function [7]. This phenomenon distorts a transmitted pulse (side lobes of residual ringing appears [8]) even though the pulse spectrum was limited to the passband of the antenna. Specially designed Vivaldi-horn antennas for lightweight UAVs practically do not have distortion of pulse response [9]. Nowadays Vivaldi-horn antennas are widely used as radar antennas on UAVs [1]-[4], [9], despite the larger construction volume and weight in relation to LPD antenna (with the corresponding bandwidth). At the same time, novel methods for designing LPD antennas [7] and hardware components, implementing corrective time delay circuits [10], [11] have been developed. These approaches significantly reduce the distortion of the pulse response of LPD antennas.

In contrast to the existing approaches, this work proposes a software-defined correction of amplitude and phase-frequency responses of conventional LPD antenna (that was used on UAV radar [8]). The proposed approach of UWB pulses synthesizing is close to the ideas described in [12], [13]. However, in [12], a nondispersive antenna was used, and the amplitude and phase-frequency responses of the antenna were not corrected. In [13], a train of 4 radio pulses was used to synthesize a nanosecond video impulse using a broadband

The investigation supported by the Russian Science Foundation and the Krasnoyarsk Regional Science Foundation, project № 22-17-20042.

dipole antenna. The amplitude and the phase of the video impulses were corrected employing hardware in four channels to eliminate the unevenness of the frequency response of antenna system.

## II. Model of Transmitter-Receiver Antenna and Calibration Method

### A. Model of Transmitter-Receiver Antenna

Let the LPDA antenna be placed in the air over the half-space in a monostatic radar configuration. The form of LPD antenna is a trapezoid with a height, large and small base of 233mm, 285mm and 95mm, respectively. Maximum of the LPD antenna pattern is oriented to nadir. The vertical position of the antenna is determined by the distance, *d*, between the flat interface (air and half-space) and the bottom end of the LPD antenna. Then, the position of the antenna phase center, *h*, (averaged over some frequency range) will be characterized by a value of $h=d+\Delta$. The vector network analyzer (VNA) assumed as an ideal SFCW radar was connected through coaxial cable to the antenna. In such configuration measured reflection coefficient, $r(f,d,\Delta)$, in some VNA calibration reference plane, can be described by the model of two-port linear network with S-parameters [14], [15]:

$$r(f,d,\Delta) = r_0(f) + \frac{G(f,d,\Delta)H(f)}{1-S_{22}(f)G(f,d,\Delta)}, \quad (1)$$

where $r_0(f)$ is the return loss of the antenna in free space (empty room), *f* is the wave frequency, $H(f)$ is the two-way (in the bistatic configuration) complex antenna transfer function (CATF), $S_{22}$ is the return loss of the wave, passing the cross-section of the antenna through the point of phase center from the side of main lobe, $G(f,d,\Delta)$ is the transfer function of the complex amplitude of a spherical wave, which propagates from a cross-section of the antenna in the point of phase center through free space and reflected back off the half-space. Transfer function $G(f,d,\Delta)$ in the model (1), can be presented in the form of:

$$G(f,d,\Delta) = R(f)g(f,d,\Delta),$$
$$g(f,d,\Delta) = \frac{1}{4\pi}\frac{e^{4\pi i\frac{f}{c}(d+\Delta)}}{2(d+\Delta)}. \quad (2)$$

Where $g(f,d,\Delta)$ is the scalar Green's function in free space [16], *R(f)* is the Fresnel reflection coefficient from half-space, *c* is the velocity of light in vacuum. Unlike the calibration process [15], here for the model (1)-(2), the spherical divergence of the wave front of the radiated and received wave will take into account using the scalar Green's function. On the other hand, neglect the constants related to the amplitude of point source, the model (2) corresponds to the exact analytical expression for Green's functions of a horizontal electric dipole above dielectric half-space, derived in the far-field approximation [17] (which is always take place for UAV flight altitudes). Such simplification of the exact analytical expression of Green's function allows proposing an amplitude-phase method for the calibration of model parameters (1) - (2), original concerning works [14], [15].

### B. Method of Antenna Calibration

It will be assumed that the condition S22=0 is met. Next, the reflection coefficients $r_m = r(f,d_m,\Delta)$ and $r_l = r(f,d_l,\Delta)$ are measured at some heights of $d_m$ and $d_l$, above flat metal surface, where $m=1,\ldots,L$, $l=1,\ldots,L$ ($m \neq l$). *L* is the total number of heights. Then, from the reduced ratio of reflection coefficients:

$$\alpha_{lm} \equiv \frac{r(f,d_l,\Delta)-r_0(f)}{r(f,d_m,\Delta)-r_0(f)} = \frac{d_m+\Delta}{d_l+\Delta}e^{4\pi i\frac{f}{c}(d_l-d_m)}, \quad (3)$$

the estimation of the reflection coefficient in "empty room" $r_0 = r(f,d\to\infty,\Delta)$ can be obtained:

$$r_0^{th}(f,\ d_l,d_m,\Delta) = \frac{r(f,d_l,\Delta)-\alpha_{lm}r(f,d_m,\Delta)}{1-\alpha_{lm}}. \quad (4)$$

From the difference in reflection coefficients $r(f,d_l,\Delta)$ and $r(f,d_m,\Delta)$, the estimation of CATF can be obtained:

$$H^{th}(f,d_l,d_m,\Delta) = -\frac{r(f,d_l,\Delta)-r(f,d_m,\Delta)}{\frac{exp(2ik_0(d_l+\Delta))}{2(d_l+\Delta)}-\frac{exp(2ik_0(d_m+\Delta))}{2(d_m+\Delta)}}. \quad (5)$$

In Equations (3)-(5), the values of $r(f,d_l,\Delta)$ and $r(f,d_m,\Delta)$ must be interpreted as measured reflection coefficients $r^{meas}(f,d_l)$ and $r^{meas}(f,d_m)$ at the corresponding heights. Equations (4) and (5) make it possible to determine the spectrum of return loss (in empty room) and CATF from two measurements of reflection coefficients at some two different heights $d_m$ and $d_l$ of antenna. However, firstly, the position of antenna phase center, $h_{m,l}$, above the metal sheet is unknown, and the value of Δ needs to be determined. Secondly, the $r_0^{th}(f,\ d_l,d_m,\Delta)$ and $H^{th}(f,d_l,d_m,\Delta)$ values found for the different pair of heights $(d_l,d_m)$ will differ. The Δ value can be determined in the course of minimizing the residual norm of the $F(\Delta)$ between the measured $r^{meas}(f,d_l)$ and calculated $r^{th}(f,d_l,\Delta)$ values of reflection coefficients at corresponding heights of $d_l$:

$$F(\Delta) = \sum_{l=1}^{L}\sum_f |r^{meas}(f,d_l) - r^{th}(f,d_l,\Delta)| \quad (6)$$

$$r^{th}(f,d_l,\Delta) = < r_0^{th}(f,\Delta) > - g(f,d_l,\Delta) < H^{th}(f,\Delta) >$$

$$\begin{matrix} <r_0^{th}(f,\Delta)> \\ <H^{th}(f,\Delta)> \end{matrix} = \frac{1}{L(L-1)}\sum_{\substack{l,m \\ l\neq m}} \begin{matrix} r_0^{th}(f,d_l,d_m,\Delta) \\ H^{th}(f,d_l,d_m,\Delta) \end{matrix}$$

where $< r_0^{th}(f,\Delta) >$ and $< H^{th}(f,\Delta) >$ are the average return loss (in empty room) and CATF, calculated for all possible combinations of different antenna heights.

## III. Result and Discussion

### A. Retrieved Spectrum of Return Loss and Transfer function of the antenna

In order to calibrate the antenna parameters, the experiment was carried out for *L*=6 antenna heights: $\vec{d}$ =(0.399m, 0.446m, 0.490m, 0.670m, 0.780m, 0.846m) above metal sheets (2m x 2m) (see Fig. 1). (These heights were measured relative to the bottom edge of the antenna.) Measurements of the reflection coefficients were performed using Agilent FieldFox 9927A vector network analyzer (VNA) over a frequency range from 400 MHz to 1.1 GHz. The VNA was connected via a 6m long coaxial cable to the LPD antenna. Before taking measurements, the VNA was warmed up for 30 minutes, and then calibrated using a

mechanical kit (Agilent 85518A Full 2-Port Calibrator, Type-N-50 Ohm).

Fig. 1. Appearance of the laboratory radar stand, in which the experiment was carried out.

In accordance with the above methodology, the minimization problem (6) was solved using the Levenberg-Marquardt algorithm [18]. Values of Δ, the functions of average return loss (in empty room) and CATF (see Fig. 2) were found.

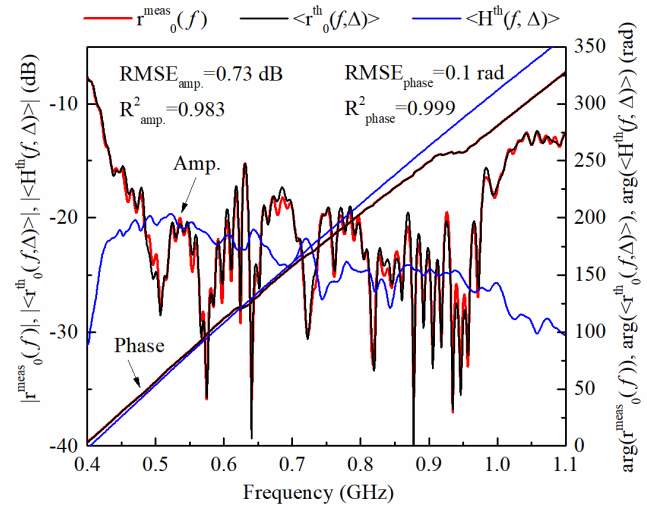


Fig. 2. Amplitude and phase of the measured and retrieved return loss, as well as the retrieved complex antenna transfer function, using the proposed method.

The phase center of the antenna is displaced from bottom edge towards the geometrical antenna center on average of Δ=10.1 cm in the frequency range from 0.4 to 1.1 GHz. Root-mean square error (RMSE) and coefficient of determination ($R^2$) between found $|<r_0^{th}(f,\Delta)>|$ and measured $|r_0^{meas}(f)|$ absolute values of reflection coefficients (in an empty room) are appeared to be RMSE=0.73dB, $R^2$=0.983 (see Fig. 2). Root-mean square error and coefficient of determination between found $arg(<r_0^{th}(f,\Delta)>)$ and measured $arg(r_0^{meas}(f))$ phases of reflection coefficients (in an empty room) are appeared to be RMSE=0.06 rad, $R^2$=0.999 (see Fig. 2).

### B. *Application of Calibrated Model of LPD Antenna for Synthesizing UWB Pulses*

The performed antenna calibration makes it possible to eliminate the distortions introduced by the antenna into the spectrum of radiated and received UWB pulses using amplitude and phase corrections of CATF $<H^{th}(f,\Delta)>$. Based on the model (1) - (2) and the Fourier transform, it is possible to obtain an expression for calculating the analytical signal $\dot{s}(t,d_l)$ of UWB pulse, which is synthesized using the LPD antenna:

$$\dot{s}(t,d_l)=\frac{\int_{f_{min}}^{f_{max}} df e^{-2\pi ift}}{\{r^{meas}(f,d_l)-<r_0^{th}(f,\Delta)>\}W_\alpha(f)}, \quad (7)$$

where $t$ is the time, $f_{min}$ and $f_{max}$ are the minimum and maximum frequency in the spectrum of synthesized UWB pulse, $W_\alpha(f)=\frac{K_\alpha(f)}{<H^{th}(f,\Delta)>}$, $K_\alpha(f)$ is the spectrum of Chebyshev window function, α is the pulsation level (in dB) outside the window bandwidth of $K_\alpha(f)$. The Chebyshev window function [19] was used to ensure the minimum duration of the synthesized pulses (for a given spectrum width) and to reduce the pulsation level relative to the main part of the pulse. Integral (7) was calculated using the Gauss interpolation quadrature formula [20]. The integration interval was divided into 40 segments, on each of which the Gaussian quadrature with 24 nodes were applied [20]. This number of partitions provided an absolute error in the calculation of the integral (7) in the time interval from 0 to 200 ns no worse than $10^{-2}$. Finally, the time shape $s(t,d_l)$ and the upper envelope $s^a(t,d_l)$ of the synthesized UWB pulse were calculated based on the formulas:

$$s(t,d_l)=2Re\,\dot{s}(t,d_l),\ s^a(t,d_l)=2|\dot{s}(t,d_l)|. \quad (8)$$

Numerical-analytical expressions (7)-(8) implement the method of synthesizing UWB pulses with correction of amplitude and phase frequency-response of the antenna.

As an example, Fig. 3 shows the time shapes of pulses calculated on the basis of formulas (7)-(8) with and without ($W_\alpha(f)\equiv 1$) correction of the antenna frequency-response. The ripple level outside the passband $f_{min}$=0.4 GHz up to $f_{max}$=1.1 GHz of the Chebyshev window function K was set equal to 30 dB. The duration of the synthesized UWB pulse using the LPD antenna and the proposed method appeared to be of 2.2 ns (see Fig. 3) (at the level of half the amplitude of the pulse envelope). The noise level outside the main part of the pulse is about -30dB (t>20ns). The correction of antenna frequency-response makes it possible to reduce the duration of the synthesized UWB pulse by more than 4.4 times compared to the radio pulse formed without correction (see Fig. 3). The arrival times of the first and second impulses (see Fig. 3, red and blue curves, respectively) are 3.25 ns and 5.63 ns. The time delay between arrivals of these UWB pulses is 2.38 ns. The height difference estimate calculated from the time delay of 2.38 ns is 0.357 m. This estimate, with an error of 1 mm, describes the difference in the heights of the antenna position when receiving the first and second pulses (see Fig. 3, red and blue curves, respectively). This good agreement found additionally indicates the efficiency of the proposed method.

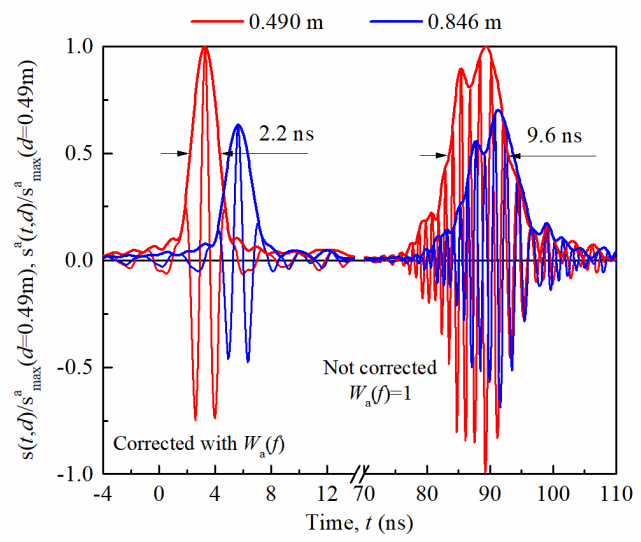


Fig. 3. Impulses radiated and received by the antenna with and without the antenna frequency-response correction.

## IV. Conclusion

In this paper, using a vector network analyzer and a transmit-receive broadband log-periodic antenna with a bandwidth from 435 MHz to 1.0 GHz (at -15 dB level), a method for synthesizing of UWB pulse with a duration of 2.2 ns is proposed (according to the level of half the amplitude of the envelope.) The correction of frequency-response of antenna, using measured complex antenna transfer function, makes it possible to reduce the duration of the synthesized UWB pulse by more than 4.4 times compared to the radio pulse generated without correction. The proposed method for synthesizing UWB pulses does not require changes in the design of the antennas and can be implemented as an additional software calibration of the antenna-feeder path.

## References


[1] K. Wu, G. A. Rodriguez, M. Zajc, E. Jacquemin, M. Clément, A. De Coster, S. Lambot, "A new drone-borne GPR for soil moisture mapping," *Remote Sensing of Environment*, vol. 235 (111456), pp. 1–9, 2019, 10.1016/j.rse.2019.111456.

[2] D. Šipoš, D. Gleich, "A Lightweight and Low-Power UAV-Borne Ground Penetrating Radar Design for Landmine Detection," *Sensors*, vol. 22(2234), 2020, 10.3390/s20082234.

[3] M. R.P. Cerquera, J. D. C. Montaño, I. Mondragón, "UAV for Landmine Detection Using SDR-Based GPR Technology," in *Robots Operating in Hazardous Environments*, IntechOpen, London, ch.2, p. 1-35, 2017, 10.5772/intechopen.69738.

[4] R. Burr, M. Schartel, P. Schmidt, W. Mayer, T. Walter, C. Waldschmidt, "Design and Implementation of a FMCW GPR for UAV-based Mine Detection," *IEEE MTT-S International Conference on Microwaves for Intelligent Mobility*, Munich, 2018, pp. 1-4, 10.1109/ICMIM.2018.8443526.

[5] Planar R60, Copper Mountain Technologies, Indianapolis, USA, [Online]. Available: https://coppermountaintech.com/vna/r60-1-port/

[6] I. Catapano, G. Gennarelli, G. Ludeno, F. Soldovieri, R. Persico, "Ground-Penetrating Radar: Operation Principle and Data Processing," in *Wiley Encyclopedia of Electrical and Electronics Engineering*, p. 1-23, 2019, 10.1002/047134608X.W8383.

[7] F. Merli, J. Zurcher, A. Freni and A. K. Skrivervik, "Analysis, Design and Realization of a Novel Directive Ultrawideband Antenna," *IEEE Transactions on Antennas and Propagation*, vol. 57, no. 11, pp. 3458-3466, 2009, 10.1109/TAP.2009.2027140.

[8] M. A. Yarlequé, S. Alvarez and H. J. Martínez, "FMCW GPR radar mounted in a mini-UAV for archaeological applications: First analytical and measurement results," *International Conference on Electromagnetics in Advanced Applications*, Verona, 2017, pp. 1646-1648, 10.1109/ICEAA.2017.8065606.

[9] R. Burr, M. Schartel, W. Mayer, T. Walter and C. Waldschmidt, "Lightweight Broadband Antennas for UAV based GPR Sensors," *15th European Radar Conference*, Madrid, 2018, pp. 245-248, 10.23919/EuRAD.2018.8546552.

[10] A. Khaleghi, H. S. Farahani and I. Balasingham, "Impulse Radiating Log-Periodic Dipole Array Antenna Using Time-Reversal Technique," *IEEE Antennas and Wireless Propagation Letters*, vol. 10, pp. 967-970, 2011, 10.1109/LAWP.2011.2167735.

[11] P. Rulikowski, J. Barrett, "Adaptive Arbitrary Pulse Shaper," *IEEE Microwave and Wireless Components Letters*, vol. 18, no. 5, pp. 356-358, 2008, 10.1109/LMWC.2008.922131.

[12] L. A. Robinson, W. B. Weir and L. Young, "Location and recognition of discontinuities in dielectric media using synthetic RF pulses," Proceedings of the IEEE, vol. 62, no. 1, pp. 36-44, 1974, 10.1109/PROC.1974.9383

[13] M.I. Finkelstein, V.A. Kutev, "Probing of Sea Ice with a Sequence of Video Pulses," Radio Engineering and Electronic Physics, vo1.17, No.10, pp. 1680-1682, 1972.

[14] V. A. Mikhnev, P. Vainikainen, "Single-reference near-field calibration procedure for step-frequency ground penetrating radar," *IEEE Transactions on Geoscience and Remote Sensing*, vol. 41, no. 1, pp. 75-80, 2003, 10.1109/TGRS.2002.808060.

[15] S. Lambot, E. C. Slob, I. van den Bosch, B. Stockbroeckx, M. Vanclooster, "Modeling of ground-penetrating Radar for accurate characterization of subsurface electric properties," *IEEE Transactions on Geoscience and Remote Sensing*, vol. 42, no. 11, pp. 2555-2568, 2004, 10.1109/TGRS.2004.834800.

[16] L. Tsang, J. A. Kong, K.-H. Ding, "Scattering of Electromagnetic Waves: Theories and Applications", John Wiley & Sons, Inc., Vol. 1, 436p, 2001.

[17] C. Y. Kee, C. Wang, "Far field approximation of half-space Green's function," IEEE International Symposium on Antennas and Propagation & USNC/URSI National Radio Science Meeting, San Diego, CA, 2017, pp. 1357-1358, 10.1109/APUSNCURSINRSM.2017.8072721.

[18] C. T. Kelley, "Iterative Methods for Optimization," SIAM Frontiers in Applied Mathematics, no 18, 180 p, 1999.

[19] F. J. Harris, "On the use of windows for harmonic analysis with the discrete Fourier transform," Proceedings of the IEEE, vol. 66, no. 1, pp. 51-83, 1978, 10.1109/PROC.1978.10837.

[20] M. Abramowitz, I.A. Stegun, "Handbook of Mathematical Functions: with Formulas, Graphs, and Mathematical Tables," National Bureau of standards, Applied mathematics series, no. 55, 1082 p, 1964.